FUSION OF MULTISUBJECT HEMODYNAMIC AND EVENT-RELATED POTENTIAL DATA USING INDEPENDENT COMPONENT ANALYSIS

V. Calhoun[1,2] and T. Adali[3]

[1]Olin Neuropsychiatry Research Center, Institute of Living, Hartford, CT 06106
[2]Yale University, New Haven, CT 06520
[3]University of Maryland, Baltimore County, Baltimore, MD 21250

ABSTRACT

Functional magnetic resonance imaging (fMRI) data provides spatially localized subcentimeter information about blood flow and oxygenation secondary to neuronal activation, but with temporal resolution on the order of seconds. Event-related potential (ERP) studies provide millimeter resolution measurements of the electric changes induced by neuronal activity, but spatial information is not well localized and suffers from an ill-posed inverse problem since there are much fewer sensors than solutions. Combining or fusing these two techniques thus has the potential to provide simultaneous higher temporal and high spatial resolution. Localization of the brain's response to infrequent, task-relevant target 'oddball' stimuli in humans has remained challenging due to the lack of a single imaging technique with good spatial and temporal resolution. In this paper, we use independent component analysis to fuse ERP and fMRI modalities to identify, for the first time in humans, the dynamics of the auditory oddball response with high spatiotemporal resolution across the entire brain. The results illuminate a new era of brain research utilizing the precise temporal information in ERPs and the high spatial resolution of fMRI.

1. INTRODUCTION

Independent component analysis (ICA), a method that maximizes the independence among components from a given mixture has been successfully used on both the fMRI and the electroencephalogram (EEG) modalities separately. The ICA approach models the data as a linear combination of spatial maps and time courses while attempting to maximize the independence between either the maps (spatial ICA) or the time courses (temporal ICA). ICA has been applied to the analysis of EEG data in which a set of signals, one from each electrode, are separated into temporally independent groups [1]. The first application of ICA to fMRI data used spatial-ICA [2] to determine spatially distinct brain networks. This practice of using temporal ICA for ERPs and spatial ICA for fMRI has now become common practice. However what has not been attempted is a joint estimation of the temporal components of the ERP response and the spatial components revealed by fMRI. Such an approach has the potential to reveal electrical sources that may not be readily visible to scalp ERPs or to expose brain regions that have participatory roles in source activity, but may not themselves be generators of the detected electrical signal [3].

In this work, we jointly performed spatial ICA of fMRI data and temporal ICA of ERP data in a group of twenty-three healthy participants in order to derive a spatiotemporal decomposition consisting of fMRI components indicating *where* the signal is changing and ERP components indicating *when* the signal is changing.

2. BACKGROUND

Though fMRI is capable of showing precise localization of hemodynamic information, the temporal resolution is on the order of seconds. Thus an approach using both electromagnetic and hemodynamic information could provide both high temporal and high spatial resolution. Despite this obvious motivation; combining these two modalities has proven technically challenging.

Several different approaches have been used previously to combine electromagnetic and hemodynamic data. Initial work focused upon constraining the electromagnetic source locations using fMRI or structural MRI data [4], thus improving the spatial estimates, but still being subject to the limited spatial resolution and poor sensitivity to deep brain structures. More recently correlations between hemodynamic and electrical activity have been observed in animals by combining intracortical recordings of neural signals with fMRI techniques [5]. In humans, correlations between fMRI and ERP peak amplitude [6] have enabled inferences to be made about both the hemodynamic and electrical sources of target detection. However there has not yet been an examination of the connection between the components of ERP waveforms (as opposed to summary measures like peak amplitude) and fMRI spatial maps. Recent work using principal component analysis (PCA) [7] has decomposed ERP waveforms into specific components corresponding to the various parts of the ERP waveform. Because scalp-recorded ERP waveforms are not particularly sensitive to deep brain structures, and because source localization methods involve solving an inverse problem which has no unique solution [8] (*i.e.,* the estimation of source locations from scalp electrodes), the precise neural generators underlying ERP components have not been identified [9]. FMRI, on the other hand, can provide precise information about the spatial characteristics of blood oxygen level dependent (BOLD) neural activity.

3. JOINT ICA OF ERP AND FMRI DATA

Joint ICA: We assume joint spatial or temporal independence of the fMRI and ERP sources, respectively, using the following generative model for the data:

$$\mathbf{x}^F = \mathbf{A}\mathbf{s}^F \text{ and } \mathbf{x}^E = \mathbf{A}\mathbf{s}^E. \quad (1)$$

For the case of two sources and two subjects, the observation vector (mixed data) for the fMRI modality and the ERP modality are:

$$\mathbf{x}^F = \begin{bmatrix} x_1^F & x_2^F \end{bmatrix}^T \text{ and } \mathbf{x}^E = \begin{bmatrix} x_1^E & x_2^E \end{bmatrix}^T \quad (2)$$

We calculate one shared linear mixing matrix given by

$$\mathbf{A} = \begin{bmatrix} a_{11} & a_{12} \\ a_{21} & a_{22} \end{bmatrix} \quad (3)$$

for the case of two sources, and $\mathbf{s}^F$ and $\mathbf{s}^E$ are the respective fMRI and ERP sources.

We use the Infomax algorithm based on the maximization of information transfer [10] (which is equivalent to maximum likelihood estimation [11]) and write the update for computing the shared unmixing matrix $\mathbf{W}$ (*i.e,.* the inverse of $\mathbf{A}$) using natural/relative gradient updates as

$$\Delta\mathbf{W} = \eta\left\{\mathbf{I} - 2\mathbf{y}^E\left(\mathbf{u}^E\right)^T - 2\mathbf{y}^F\left(\mathbf{u}^F\right)^T\right\}\mathbf{W}, \quad (4)$$

where

$$\mathbf{y}^E = g\left(\mathbf{u}^E\right),\ \mathbf{y}^F = g\left(\mathbf{u}^F\right), \quad (5)$$

$$\text{and } g(x) = 1/(1+e^{-x}) \quad (6)$$

is the nonlinearity, which is chosen as the sigmoid function.

Spatiotemporal Reconstruction. Even though the joint components (*e.g.,* as shown in Figure 3), provide a useful summary, they do not show clearly how these components interact with one another. To accomplish this task, we compute spatiotemporal "snapshots" of the significant components in two ways. First, we display all the ERP components, and compute a linear combination of the fMRI components weighted by their joint ERP time courses for a specific point in time. If the N spatial (fMRI) and temporal (ERP) components are written as

$$\mathbf{T} = \begin{bmatrix} \mathbf{t}_1 & \dots & \mathbf{t}_N \end{bmatrix}, \text{and } \mathbf{S} = \begin{bmatrix} \mathbf{s}_1 & \dots & \mathbf{s}_N \end{bmatrix}, \quad (7)$$

we can compute the fMRI movie as $\mathbf{M}_F = |\mathbf{T}|\mathbf{S}^T$ —the absolute value is needed since the joint components are fused using a single weight parameter, thus a change in the amplitude of the fMRI component is directly linked to change in the ERP component by this parameter. Likewise we compute an estimated ERP time course for a given voxel by computing $\mathbf{M}_F = \mathbf{T}|\mathbf{S}|^T$, which will be discussed in more detail in the results section.

4. FMRI/ERP EXPERIMENT

Participants and Task. Participants were recruited via advertisements, presentations at local universities, and by word-of-mouth. Twenty-three healthy participants (15 male, 8 female, Age 41±14 years) provided written, informed, IRB-approved consent at Hartford Hospital and were compensated for their participation. The auditory oddball task (AOD) consists of detecting an infrequent sound within a series of regular and different sounds. The task consisted of two runs of auditory stimuli presented to each participant by a computer stimulus presentation system via insert earphones embedded within 30 dB sound attenuating MR compatible headphones (Figure 1).

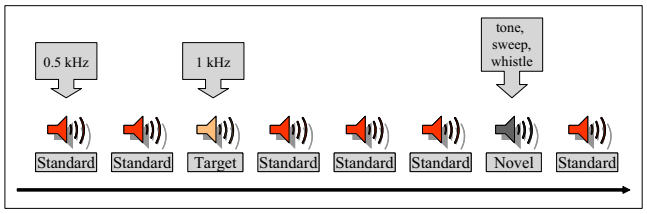

Figure 1: Auditory oddball event-related fMRI task.

The target and novel stimuli each occurred with a probability of 0.10; the non-target stimuli occurred with a probability of 0.80. The stimulus duration was 200 ms with an 800, 1300, or 1800 ms inter-stimulus interval. The stimulus paradigm, data acquisition techniques, and previously found stimulus-related activation are described more fully elsewhere [12].

Data acquisition. FMRI and ERP data were acquired on the same day in two different sessions, using identical stimuli and counterbalanced between individuals, at the Olin Neuropsychiatry Research Center at the Institute of Living. The fMRI data were collected on a Siemens Allegra 3T dedicated head scanner equipped with 40mT/m gradients and a standard quadrature head coil. The functional scans were acquired using gradient-echo echo-planar-imaging with the following parameters (repeat time (TR)=1.50s, echo time (TE)=27ms, field of view=24cm, acquisition matrix=64×64, flip angle=70°, voxel size=3.75×3.75×4mm, gap=1mm, 29 slices, ascending acquisition). Six "dummy" scans were performed at the beginning to allow for longitudinal equilibrium, after which the paradigm was automatically triggered to start by the scanner. The ERP data was collected using an SA bioelectric amplifier system capable of amplifying electrical activity from 64 separate single-ended channels. Amplifiers were connected to a 16-bit A/D conversion using a custom program (Digitize) implemented on a Pentium II micro-computer running Solaris for Intel. The Digitize program records EEG data and all stimulus and behavioral response codes for later analysis.

Preprocessing. FMRI data were preprocessed using the software package SPM2 [13]. ICA was used to remove ocular artifacts from the EEG data [14]. Data were then filtered with a 20hz high pass filter and ERPs were constructed for trials in which participants correctly identified target stimuli. Data from midline central site Cz was included in the ICA fusion analyses because it appeared to be the best single channel to detect both anterior and posterior sources (results were nearly identical when scalp site Pz was used instead of Cz).

Component Estimation. The number of independent components in the joint data was estimated to be twelve using the minimum description length as the information-theoretic criterion [15]. Independent components were

estimated, and ranked by their contribution to the average ERP time courses by first regressing the components onto the average ERP data, then computing the maximum absolute peak of the fitted time courses. Components which contributed greater than unity standard deviation were interpreted (*all* components are shown in the ERP plots for Figure 4; regions in the fMRI component were scaled to Z values and a voxel was colorized if it was greater than Z=3.5). A leave one out cross-validation approach was used to assess the robustness of the results; mean results are reported.

5. RESULTS

Performance on the auditory oddball task for the ERP and fMRI sessions was nearly identical. Mean and standard deviations are reported for a) reaction time (fMRI 430.7±90.4 ms; ERP 431.5±93.6 ms, p>0.9 paired t-test) and b) accuracy for target detection (fMRI 99.5±0.01 percent; ERP 99.5±0.02 percent, p>0.99 paired t-test).

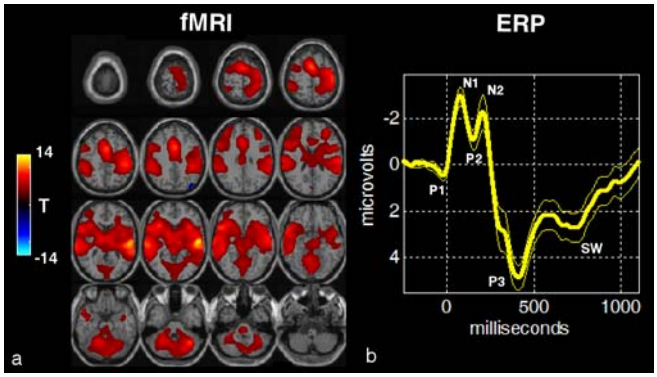

Figure 2: Group fMRI (left) and ERP (right) results for the target response.

Group averaged fMRI (Figure 2a) and ERP (Figure 2b) results are shown for the target stimuli and are consistent with previous results [16]. The fMRI data for targets activates a large amount of the brain, with local maxima in bilateral temporal lobes, inferior parietal lobe, subcortical structures such as thalamus, and motor planning and execution regions, replicating our previous work [12]. The ERP data contains the expected positive and negative peaks, N1, N2, P1, P2, P3, and slow wave (SW), (marked on the figure).

The spatial and temporal joint components for the significant components are presented in Figure 3a. Significant regions of activation for the fMRI maps are shown on the left and the average ERP time course (in yellow; on all plots) is plotted along with the components (in cyan). The ERP time courses correspond remarkably well to distinct peaks present on the average time courses. Additionally, when viewed together with the fMRI maps, the spatiotemporal dynamics of the auditory oddball target response are visible. Such a view provides a useful parameterization of the oddball response. For example, the N1 peak in Figure 3 is showing prominent activation in thalamic and primary and secondary auditory temporal lobe regions, as well as more discrete activation in several other brain regions including the supplemental motor area. Also visible for this waveform is a late negative peak.

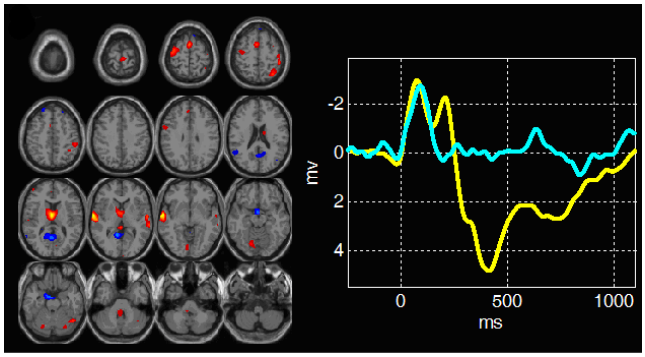

Figure 3: One of the six joint ERP and fMRI components which loaded onto the ERP time courses significantly. The fMRI maps are thresholded at |Z|>3.5 for display purposes. The average target-related ERP time course (shown also in Figure 2b) is shown in yellow and the ERP component is plotted in cyan.

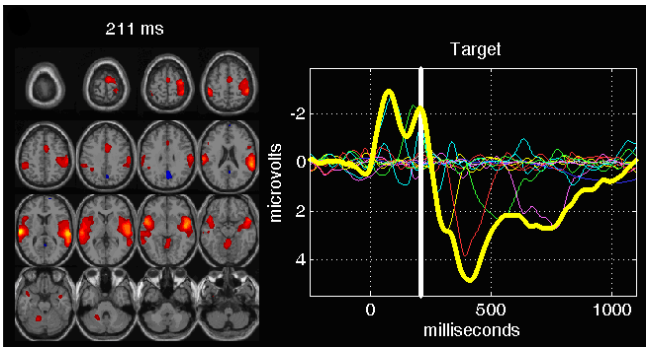

Figure 4: On the left is shown a linear combination of the fMRI maps, weighted by the ERP part of the component at a specific point in time. On the right is shown all of the estimated ERP components (the six significant ones are easily visible above the others). Such a display provides a dynamic way to visualize the results (see also movies at: http://www.nrc-iol.org/mialab/results.htm).

The ICA decomposition can be used to create a full spatiotemporal movie to more clearly reveal the dynamic interplay between the components. Figure 4 shows six "snapshots" for the movie created for the target stimuli (full movie available at http://www.nrc-iol.org/mialab/results.htm). On the left of the snapshot is shown a linear sum of the individual fMRI maps (Figure 3), weighted by their respective ERP time courses at the time indicated above the figure (e.g. 84ms). On the right of each snapshot the average ERP waveform is again plotted as are all estimated ERP components (the six significant ones are easily visible above the flat baseline). During the peak of the second ERP component, the N2, hemodynamic activity in both anterior superior temporal gyrus (a heteromodal sensory association region) and posterior middle/superior temporal gyrus (secondary auditory cortex) is visible. The first substantial positive component (the P3a) is fused with

hemodynamic activity in multiple frontal and parietal lobe regions, in addition to bilateral temporal lobe regions.

6. DISCUSSION

We show, for the first time, a spatiotemporal reconstruction of the normal human brain's response to a well-studied auditory oddball task with high temporal and spatial resolution, using a fusion of electromagnetic and hemodynamic data. Recent work, examining correspondence between these two very different types of data has showed promising results [5,17] and suggests that methods combining the strengths of both techniques (temporal resolution for ERP and spatial resolution/localization for fMRI) may provide new insights into human brain function. By taking advantage of inter-participant co-variation between the ERP and fMRI data, a connection can be made between the two by 'fusing' temporal components of the ERP time courses to spatial components of the fMRI images.

This provides a significant advantage over using fMRI or ERP separately. We focus upon the strengths of both techniques by fusing together the hemodynamic spatial information in the fMRI data with the electromagnetic temporal information in the ERP data by using the joint constraints of temporal (ERP) and spatial (fMRI) independence. Specifically, the independence between joint ERP and fMRI components is maximized while the inter-subject covariation for the fused times (ERP) and positions (fMRI) is modeled by the linear mixing parameters.

Results show, for task-relevant infrequent target stimuli, sources including primary and secondary auditory cortex and thalamus with early peak ERP responses. Later responses occur in auditory association and parietal cortex, motor execution, and then posterior temporal lobe whereas medial frontal, and brainstem regions show peaks during the P3 portion of the ERP response. Bilateral temporal lobe regions also showed a late negative peak.

In summary, we have used a combination of electrical and hemodynamic data to visualize, in humans, the neural systems involved during different portions of the auditory target detection response. Deep brain structures, which are likely participatory in the target response, but are not readily detectable with scalp ERP alone, were also implicated in our results. This work demonstrates that data fusion techniques can be successfully applied to joint ERP and fMRI data to reveal unique information that cannot be evaluated in either technique alone.

7. ACKNOWLEDGMENT

The authors would like to thank Olin Center staff for their help with data collection. This research was supported in part by the National Institutes of Health under grant numbers R01 EB 000840 and R01 EB 005846.

8. REFERENCES

[1] S. Makeig, T. P. Jung, A. J. Bell, D. Ghahremani, and T. J. Sejnowski, "Blind Separation of Auditory Event-Related Brain Responses into Independent Components," *Proc. Natl. Acad. Sci.*, vol. 94, pp. 10979-10984, 1997.

[2] M. J. McKeown, S. Makeig, G. G. Brown, T. P. Jung, S. S. Kindermann, A. J. Bell, and T. J. Sejnowski, "Analysis of FMRI Data by Blind Separation Into Independent Spatial Components," *Hum. Brain Map.*, vol. 6, pp. 160-188, 1998.

[3] E. Martinez-Montes, P. A. Valdes-Sosa, F. Miwakeichi, R. I. Goldman, and M. S. Cohen, "Concurrent EEG/FMRI Analysis by Multiway Partial Least Squares," *NeuroImage*, vol. 22, pp. 1023-1034, 2004.

[4] A. M. Dale, A. K. Liu, B. R. Fischl, R. L. Buckner, J. W. Belliveau, J. D. Lewine, and E. Halgren, "Dynamic Statistical Parametric Mapping: Combining FMRI and MEG for High- Resolution Imaging of Cortical Activity," *Neuron*, vol. 26, pp. 55-67, 2000.

[5] N. K. Logothetis, J. Pauls, M. Augath, T. Trinath, and A. Oeltermann, "Neurophysiological Investigation of the Basis of the FMRI Signal," *Nature*, vol. 412, pp. 150-157, 2001.

[6] D. H. Mathalon, S. L. Whitfield, and J. M. Ford, "Anatomy of an Error: ERP and FMRI," *Biol. Psychol.*, vol. 64, pp. 119-141, 2003.

[7] J. Kayser and C. E. Tenke, "Optimizing PCA Methodology for ERP Component Identification and Measurement: Theoretical Rationale and Empirical Evaluation," *Clin. Neurophysiol.*, vol. 114, pp. 2307-2325, 2003.

[8] E. Halgren and K. Marinkovic, General principles for the physiology of cognition as suggested by intracranial ERPs. In: *Recent advances in event-related brain potential research*, eds. C.Ogura, Y.Koga, and M.Shimokochi. Amsterdam ; New York: Elsevier, 1996.pp. 1072-1084.

[9] S. Baillet and L. Garnero, "A Bayesian Approach to Introducing Anatomo-Functional Priors in the EEG/MEG Inverse Problem," *IEEE Trans. Biomed. Eng*, vol. 44, pp. 374-385, 1997.

[10] A. J. Bell and T. J. Sejnowski, "An Information Maximisation Approach to Blind Separation and Blind Deconvolution," *Neural Comput.*, vol. 7, pp. 1129-1159, 1995.

[11] J. F. Cardoso, "Infomax and Maximum Likelihood for Source Separation," *IEEE Letters on Signal Processing*, vol. 4, pp. 112-114, 1997.

[12] K. A. Kiehl, M. Stevens, K. R. Laurens, G. D. Pearlson, V. D. Calhoun, and P. F. Liddle, "An Adaptive Reflexive Processing Model of Neurocognitive Function: Supporting Evidence From a Large Scale (n=100) FMRI Study of an Auditory Oddball Task," *NeuroImage*, vol. 25, pp. 899-915, 2005.

[13] K. J. Worsley and K. J. Friston, "Analysis of FMRI Time-Series Revisited--Again," *NeuroImage*, vol. 2, pp. 173-181, 1995.

[14] T. P. Jung, S. Makeig, C. Humphries, T. W. Lee, M. J. McKeown, V. Iragui, and T. J. Sejnowski, "Removing Electroencephalographic Artifacts by Blind Source Separation," *Psychophysiology*, vol. 37, pp. 163-178, 2000.

[15] M. Wax and T. Kailath, "Detection of Signals by Information Theoretic Criteria," *IEEE Trans. Acous. Speech, and Sig. Proc.*, vol. 33, pp. 387-392, 1985.

[16] E. Halgren, K. Marinkovic, and P. Chauvel, "Generators of the Late Cognitive Potentials in Auditory and Visual Oddball Tasks," *Electroencephalogr. Clin. Neurophysiol.*, vol. 106, pp. 156-164, 1998.

[17] S. G. Horovitz, P. Skudlarski, and J. C. Gore, "Correlations and Dissociations Between BOLD Signal and P300 Amplitude in an Auditory Oddball Task: a Parametric Approach to Combining FMRI and ERP," *Magn Reson. Imaging*, vol. 20, pp. 319-325, 2002.